Performance Evaluation of an Inverter-Based Microgrid Under Cyberattacks

Conference Paper · June 2020

DOI: 10.1109/SoSE50414.2020.9130524

4 authors:

Ardavan Mohammadhassani
Virginia Polytechnic Institute and State University
7 PUBLICATIONS **12** CITATIONS
SEE PROFILE

Armin Teymouri
Washington State University
9 PUBLICATIONS **73** CITATIONS
SEE PROFILE

Ali Mehrizi-Sani
Virginia Polytechnic Institute and State University
119 PUBLICATIONS **4,272** CITATIONS
SEE PROFILE

Kambiz Tehrani
ESIGELEC
34 PUBLICATIONS **323** CITATIONS
SEE PROFILE

Performance Evaluation of an Inverter-Based Microgrid Under Cyberattacks

Ardavan Mohammadhassani
The Bradley Department of ECE
Virginia Tech
Blacksburg, VA 24061
ardavanmh93@vt.edu

Armin Teymouri
School of EECS
Washington State University
Pullman, WA 99164
armin.teymouri@wsu.edu

Ali Mehrizi-Sani
The Bradley Department of ECE
Virginia Tech
Blacksburg, VA 24061
mehrizi@vt.edu

Kambiz Tehrani
ESIGELEC
Normandy University
Rouen, France
kambiz.tehrani@esigelec.fr

***Abstract*—Distributed renewable energy resources (DER) are interfaced in a microgrid through power electronic converters (PEC). PECs utilize different types of sensors for their reliable and stable operation. However, as the ratings of a DER increase, its interfacing PEC becomes more sophisticated requiring more sensors. This will make PECs more vulnerable to sensor malfunctions, which may be caused by cyberattacks. This paper analyzes the performance of a microgrid under sensor malfunction attacks in PECs for different scenarios in MATLAB/SIMULINK and provides a final evaluation based on the acquired results.**

***Index Terms*—Cyber-physical systems, inverters, microgrids, renewable energy sources, sensor systems**

I. Introduction

Distributed energy resources (DER) are being increasingly integrated within the distribution system in the form of a microgrid [1]–[4]. DERs of a microgrid are interfaced via power electronic converters (PEC). In order to enable the reliable and stable control of microgrids, the PECs require different types of DC and AC sensors [5], [6]. This will make the PECs more vulnerable to sensor malfunctions and failures which can be caused by cyberattacks. This will put the operation of the microgrid at risk. Thus, it is of significant importance to study and evaluate the operation of microgrids under PEC sensor malfunctions [7], [8].

Among various PEC topologies, the cascaded H-bridge converter (CHB) is an attractive topology for interfacing DERs [9]–[13]. This is due to its simple topology, modularity, DC-bus isolation, and H-bridge (HB) maximum power point tracking capability. The CHB is constructed by connecting a number of HBs in series. Hence, as the ratings of a DER increase, the number of HBs will also increase. Therefore, the CHB will require more sensors for its reliable operation [14]. This will increase the risk of sensor malfunctions in CHBs which will affect the operation of DERs and the microgrid. However, very little research has been carried out on this matter [15]. Reference [16] is probably the only work that addresses the sensor malfunction problem in CHBs. This work detects single sensor malfunctions and replaces the sensor output with its estimate.

Efforts have been made to enable the unbalanced operation of CHBs. An HB-independent MPPT controller is proposed in [17]. A modified CHB topology is proposed in [18] to mitigate the power mismatch between HBs. Injecting zero sequence currents and voltages is investigated in [19]. However, none of these works address the unbalanced operation of CHBs due to sensor malfunctions.

One other way to make the CHB system more resilient towards sensor malfunctions is to reduce the number of required sensors by proposing new CHB topologies and control systems. Reference [20] introduces a new sensorless PWM control based on a new CHB topology. A modified MPPT algorithm is proposed in [19] for reducing the number of sensors and components. A method in [21] to remove both voltage and current sensors on the DC bus of CHBs. Although these methods help to make the system more resilient towards sensor and component failures, they do not address the sole problem of sensor malfunction.

This paper studies the operation of microgrids under sensor malfunctions in CHBs during different conditions. The sensor fault-ride-through method proposed in [16] is discussed first. A 9-level CHB system with four PV panels is created in MATLAB/SIMULINK for simulation purposes. Simulations are performed under different CHB operating conditions to investigate the effect of sensor malfunction on the operation of the CHB system.

The rest of this paper is structured as follows. Section II describes the method proposed in [16] for sensor malfunction detection and ride-through. Section III describes the study system. Section IV provides a discussion on simulation results. Finally, conclusions are provided in Section V.

II. A Brief Review on Detection of Sensor Malfunction and Ride-Through

This sections provides a brief review of the method proposed in [16] for detecting sensor malfunctions in CHBs and providing a seamless operation. In this method, the output of all sensors is estimated using a state estimation block regardless of their health status. During sensor failures, the output of the sensor is replaced by its estimate value. Hence, this method increases the redundancy and resiliency of the CHB system towards sensor malfunctions while keeping the required number of components. A 9-level CHB with four HB modules is considered.

978-1-7281-8050-2/20/$31.00 ©2020 IEEE

The method devised in [16] is summarized using a flowchart shown in Fig. 1. Only single sensor malfunctions are considered in this method. The first step in this method is to calculate the AC-side currents of each HB. This value is calculated based on (1). An integrator with feedback is used to deal with the DC value in (1).

$$i_{ac} = \frac{1}{L_o} \int_T \left(\sum_1^4 M_i V_{C,i} - R_o i_{ac} - V_o \right) dt \qquad (1)$$

where, L_o is the AC-side inductance, M_i is the modulation index for each HB, $V_{C,i}$ is the capacitor voltage of the DC-side for each HB, R_o is the output resistance, i_{ac} is the AC-side current, and V_o is the AC-side voltage.

The second method to calculate the AC-side current would be to take the measurements from the DC-side of each HB and calculate the AC-side current using (2). In this equation, the modulation index cannot be zero. Hence, the measurements from the HB operating in PWM mode are removed. The four currents are merged into three signals by removing the signal from the HB in PWM mode. This is done to get proper output current signals.

$$i_{ac,\mathrm{HB}_j} = \frac{1}{M_{\mathrm{HB}_j}} \left(i_{DC,\mathrm{HB}_j} - C_{\mathrm{HB}_j} \frac{dV_{C_{\mathrm{HB}_j}}}{dt} \right) \qquad (2)$$

In order to detect a falsified signal, three-by-three averaging technique is performed on the ac-side current signals. A falsified signal is detected by calculating the error between the signal and the average value. The error bound is set to 5%. After a falsified signal is detected, it is omitted from the set of three signals and averaging is performed again without the falsified signal. After this step, the faulty HB is detected and its modulation scheme is changed to either $+1$ or -1.

III. Study System

The study system is shown in Fig. 2. A 9-level CHB system interfaces a PV system with the power system. The CHB system consists of 4 HBs. Each HB interfaces a PV panel. There are two sensors for the DC-side and three sensors for the AC-side. The DC-side sensors include voltage and current sensors while the AC-side sensors include the AC terminal voltage sensor, AC current sensor, and AC grid voltage sensor. Hence, the CHB system includes 20 sensors in total. The control system designed in [16] for each PV panel is shown in Fig. 3. The MPPT system generates the reference capacitor voltage which is fed through a controller system to generate the reference d-axis voltage. The q-axis reference current is generated by a reactive power control block which is then fed through a controller to generate the q-axis reference output voltage. The modulation system uses the reference voltage and current to control the CHB system. Two case studies are designed in this paper to evaluate the operation of the simulated system under sensor malfunctions in the CHB system. The first case investigates the effect of AC-side current sensor malfunction with unequal power generation among the HBs. In the second case, the effect of undetected DC-side voltage sensor malfunctions is shown in the capacitor voltages of the faulty HB.

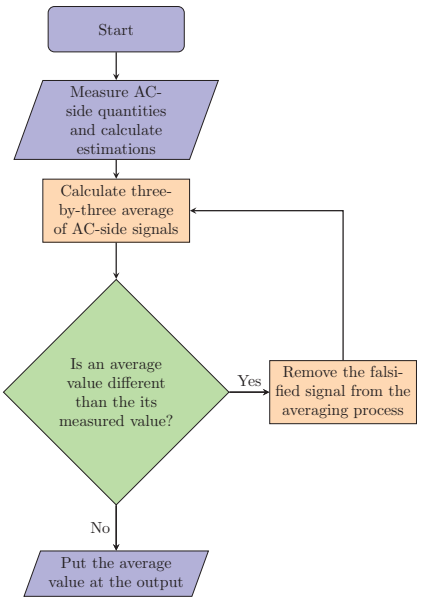

Fig. 1. Flowchart of the sensor malfunction detection and ride-through scheme proposed in [16]

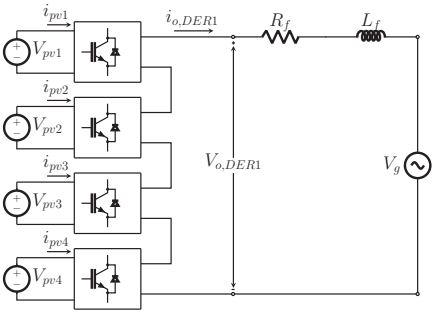

Fig. 2. The simulated system in MATLAB/SIMULINK.

IV. Simulation Results and Discussions

In this section, two case studies are carried out in SIMULINK to analyze the effect of sensor malfunction in the 9-level CHB system. Simulations are performed on a low-power CHB system to obtain correlation between simulation and experimental results.

Case 1: Effect of AC-Side Current Sensor Malfunction with Unequal Generation among HBs

The DC voltages of the HBs during unequal power generation are shown in Fig. 4. The DC voltages of the PV panels are different which can be due to environmental conditions such as partial shading. The results show that DC voltages are properly controlled during sensor malfunctions.

The output power of the PV panels are shown in Fig. 5. Due to unequal DC input voltages of the HBs, the output power of the HBs are also different. The output powers show that

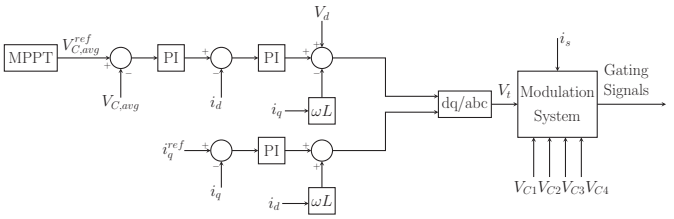

Fig. 3. The MPPT control system for each PV unit [16].

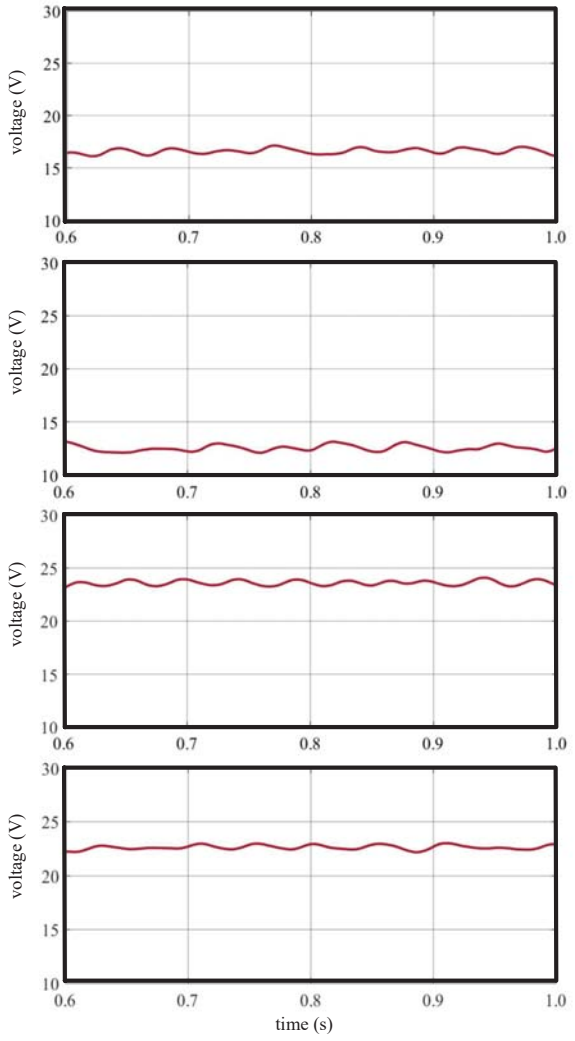

Fig. 4. DC-side voltages with unequal power generations in different HBs.

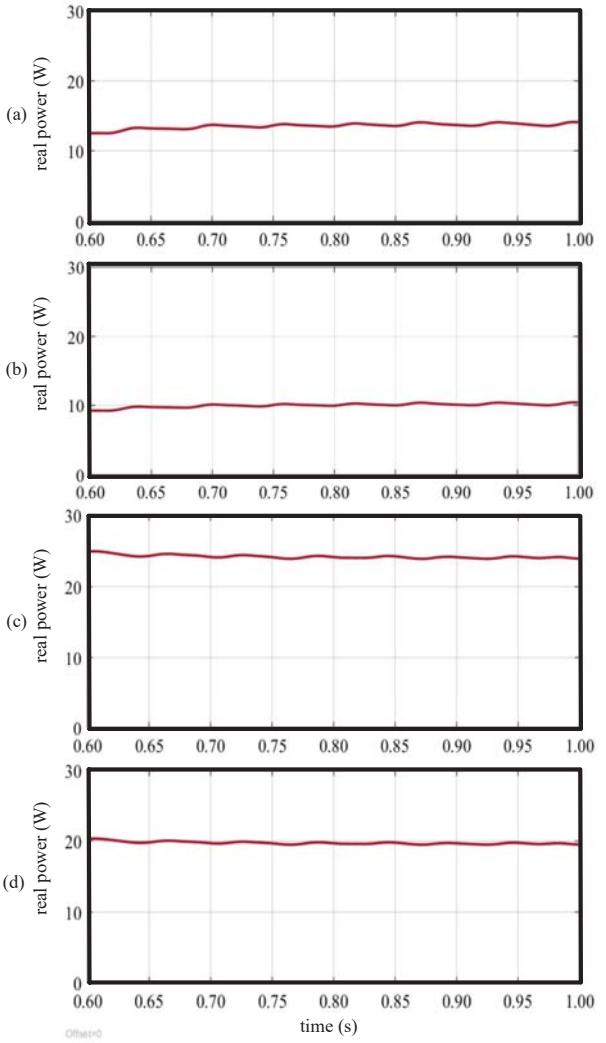

Fig. 5. Output power of HBs with unequal DC-side voltages.

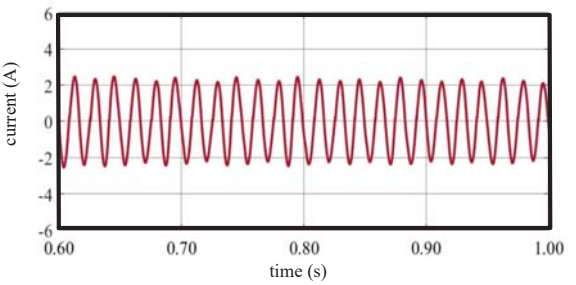

Fig. 6. Output current with unequal power generations.

the correct operation of the PV system was achieved during sensor malfunction.

The AC-side current of the PV system is shown in Fig. 6. The current is sinusoidal and is successfully controlled when sensor malfunction occurs.

The output voltage of the CHB system is shown in Fig. 7. The AC output voltage goes through changes at the instant of sensor malfunction. However, it follows the correct switching patter after the output of the faulty sensor is replaced with its estimation and the PWM system changes the switching pattern.

In summary, simulation results demonstrated that the method proposed in [16] was successfully able to control the PV system and the microgrid during AC-side current sensor malfunction when the PV panels were generating unequal

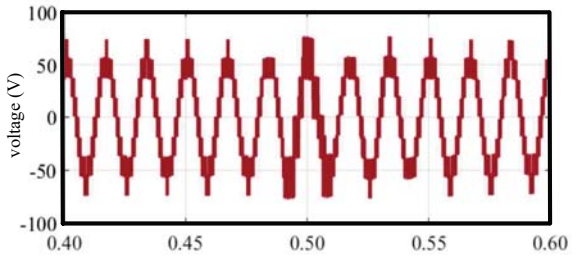

Fig. 7. The output voltage of the CHB system during sensor malfunction.

voltages and powers.

Case 2: Effect of Undetected DC-Link Voltage Sensor Malfunctions on DC-Side Voltages

In this case, simulation is run when an undetected DC-link voltage sensor malfunction occurs in HB4. The DC capacitor voltages of the HBs are shown in Fig. 8. It is demonstrated that the DC voltages become unstable. This is because the capacitor voltage of HB4 starts to decrease and reverses its polarity. The change in polarity is very dangerous when electrolytic capacitors are used. A reversed voltage polarity will increase the temperature of the capacitor and cause an explosion.

The reason behind the decrease in the capacitor voltage of HB4 can be explained by referring to the control system shown in Fig. 3. When the DC voltage sensor of HB4 is lost and the malfunction is not detected, the DC average voltage decreases. However, the reference DC average voltage is still constant. Thus, the controller tries to increase i_d and V_d to control the CHB system. This will cause the capacitor of HB4 to release excessive energy and reduce its voltage until it goes below zero.

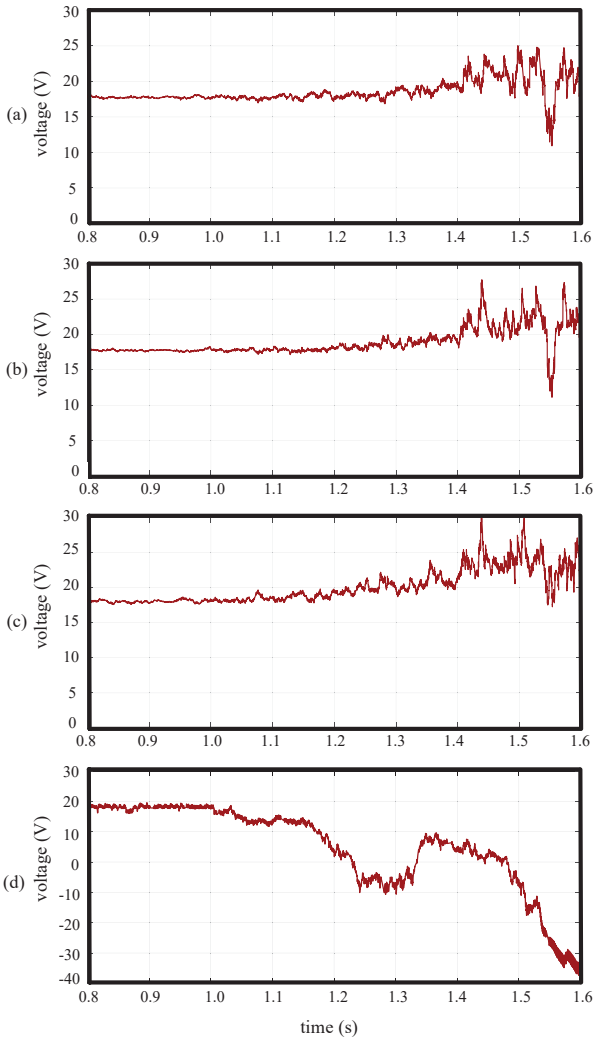

Fig. 8. DC-side voltages during undetected sensor malfunction in HB4.

V. Conclusions

This paper evaluates the performance of a 9-level CHB system interfacing a PV system during sensor malfunctions. A 9-level CHB system interfacing 4 PV panels was modeled in MATLAB/SIMULINK for simulation. The studied sensor malfunction detection and ride-through method allows the CHB system to maintain its normal operation during unequal power generation by the PV panels. It was also shown that a sensor malfunction can be destructive to the PV system if undetected.

References

[1] R. H. Lasseter, "Smart distribution: Coupled microgrids," *Proc. IEEE*, vol. 99, no. 6, pp. 1074–1082, June 2011.

[2] R. Uluski, J. Kumar, S. S. M. Venkata, D. Vishwakarma, K. Schneider, A. Mehrizi-Sani, R. Terry, and W. Agate, "Microgrid controller design, implementation, and deployment: A journey from conception to implementation at the philadelphia navy yard," *IEEE Power and Energy Magazine*, vol. 15, no. 4, pp. 50–62, July 2017.

[3] S. Leitner, M. Yazdanian, A. Mehrizi-Sani, and A. Muetze, "Small-signal stability analysis of an inverter-based microgrid with internal model-based controllers," *IEEE Trans. Smart Grid*, vol. 9, no. 5, pp. 5393–5402, Sep. 2018.

[4] D. E. Olivares, A. Mehrizi-Sani, A. H. Etemadi, C. A. Cañizares, R. Iravani, M. Kazerani, A. H. Hajimiragha, O. Gomis-Bellmunt, M. Saeedifard, R. Palma-Behnke, G. A. Jiménez-Estévez, and N. D. Hatziargyriou, "Trends in microgrid control," *IEEE Trans. Smart Grid*, vol. 5, no. 4, pp. 1905–1919, July 2014.

[5] S. Saadatmand, M. S. Sanjari Nia, P. Shamsi, and M. Ferdowsi, "Dual heuristic dynamic programing control of grid-connected synchronverters," in *2019 North American Power Symposium (NAPS)*. IEEE, 2019, pp. 1–6.

[6] S. Saadatmand, M. S. Sanjari Nia, P. Shamsi, M. Ferdowsi, and D. Wunsch, "Heuristic dynamic programming for adaptive virtual synchronous generators," in *2019 North American Power Symposium (NAPS)*. IEEE, 2019, pp. 1–6.

[7] A. Teymouri, A. Mehrizi-Sani, and C. Liu, "Cyber security risk assessment of solar pv units with reactive power capability," in *IECON 2018 - 44th Annual Conference of the IEEE Industrial Electronics Society*, Oct 2018, pp. 2872–2877.

[8] A. Gholami, M. Mousavi, A. K. Srivastava, and A. Mehrizi-Sani, "Cyber-physical vulnerability and security analysis of power grid with hvdc line," in *2019 North American Power Symposium (NAPS)*, Oct 2019, pp. 1–6.

[9] J. Chavarria, D. Biel, F. Guinjoan, C. Meza, and J. J. Negroni, "Energy-balance control of pv cascaded multilevel grid-connected inverters under level-shifted and phase-shifted pwms," *IEEE Trans. Ind. Electron.*, vol. 60, no. 1, pp. 98–111, Jan 2013.

[10] S. Ziaeinejad, Y. Sangsefidi, and A. Mehrizi-Sani, "A generalized switching strategy and capacitor sizing algorithm for granular multilevel converters," *IEEE Trans. Ind. Electron.*, vol. 65, no. 6, pp. 4443–4453, June 2018.

[11] A. MohammadHassani and E. Babaei, "Exchange market algorithm for selective harmonic elimination in cascaded multilevel inverters," in *13th International Conference on Theory and Application of Fuzzy Systems and Soft Computing — ICAFS-2018*, R. A. Aliev, J. Kacprzyk, W. Pedrycz, M. Jamshidi, and F. M. Sadikoglu, Eds. Cham: Springer International Publishing, 2019, pp. 594–601.

[12] A. M. Hassani, S. I. Bektas, and S. H. Hosseini, "Modular multilevel converter circulating current control using model predictive control combined with genetic algorithm," *Procedia Computer Science*, vol. 120, pp. 780 – 787, 2017, 9th International Conference on Theory and Application of Soft Computing, Computing with Words and Perception, ICSCCW 2017, 22-23 August 2017, Budapest, Hungary. [Online]. Available: http://www.sciencedirect.com/science/article/pii/S1877050917325206

[13] S. Saadatmand, M. S. Sanjari Nia, P. Shamsi, M. Ferdowsi, and D. Wunsch, "Neural network predictive controller for grid-connected virtual synchronous generator," in *2019 North American Power Symposium (NAPS)*. IEEE, 2019, pp. 1–6.

[14] S. Vahid, H. Rastegar, S. H. Fathi, and M. Jedari, "A comprehensive comparison between three different control strategies for four-leg active power filters," in *2016 4th International Symposium on Environmental Friendly Energies and Applications (EFEA)*, Sep. 2016, pp. 1–7.

[15] A. Teymouri, P. M. Shabestari, M. Mousavi, and A. Mehrizi-Sani, "Feedforward accurate power sharing and voltage control for multi-terminal hvdc grids," in *IECON 2019 - 45th Annual Conference of the IEEE Industrial Electronics Society*, vol. 1, Oct 2019, pp. 4819–4824.

[16] A. Teymouri and A. Mehrizi-Sani, "Sensor malfunction detection and mitigation strategy for a multilevel photovoltaic converter," *IEEE Trans. Energy Convers.*, Accepted for Publication.

[17] M. Miranbeigi and H. Iman-Eini, "Hybrid modulation technique for grid-connected cascaded photovoltaic systems," *IEEE Trans. Ind. Electron.*, vol. 63, no. 12, pp. 7843–7853, Dec 2016.

[18] C. D. Townsend, Y. Yu, G. Konstantinou, and V. G. Agelidis, "Cascaded h-bridge multilevel pv topology for alleviation of per-phase power imbalances and reduction of second harmonic voltage ripple," *IEEE Trans. Power Electron.*, vol. 31, no. 8, pp. 5574–5586, Aug 2016.

[19] Y. Yu, G. Konstantinou, C. D. Townsend, and V. G. Agelidis, "Comparison of zero-sequence injection methods in cascaded h-bridge multilevel converters for large-scale photovoltaic integration," *IET Renew. Power Gener.*, vol. 11, no. 5, pp. 603–613, 2017.

[20] N. Sandeep and U. R. Yaragatti, "Design and implementation of a sensorless multilevel inverter with reduced part count," *IEEE Trans. Power Electron.*, vol. 32, no. 9, pp. 6677–6683, Sep. 2017.

[21] G. Farivar, B. Hredzak, and V. G. Agelidis, "A dc-side sensorless cascaded h-bridge multilevel converter-based photovoltaic system," *IEEE Trans. Ind. Electron.*, vol. 63, no. 7, pp. 4233–4241, July 2016.